

Assessing the spatial distribution of coral bleaching using small unmanned aerial systems

Joshua Levy¹  · Cynthia Hunter² · Trent Lukaczyk^{3,4} · Erik C. Franklin⁵

Received: 7 May 2017 / Accepted: 29 January 2018
© The Author(s) 2018. This article is an open access publication

Abstract Small unmanned aerial systems (sUAS) are an affordable, effective complement to existing coral reef monitoring and assessment tools. sUAS provide repeatable low-altitude, high-resolution photogrammetry to address fundamental questions of spatial ecology and community dynamics for shallow coral reef ecosystems. Here, we qualitatively describe the use of sUAS to survey the spatial characteristics of coral cover and the distribution of coral bleaching across patch reefs in Kāneʻohe Bay, Hawaii, and address limitations and anticipated technology advancements within the field of UAS. Overlapping sub-decimeter low-altitude aerial reef imagery collected during the 2015 coral bleaching event was used to construct high-resolution reef image mosaics of coral bleaching responses on four Kāneʻohe Bay patch reefs, totaling ~ 60,000 m². Using sUAS imagery, we determined that pale, bleached

and healthy corals on all four reefs were spatially clustered. Comparative analyses of data from sUAS imagery and in situ diver surveys found as much as 14% difference in coral cover values between survey methods, depending on the size of the reef and area surveyed. When comparing the abundance of unhealthy coral (paled and bleached) between sUAS and in situ diver surveys, we found differences in cover from 1 to 49%, depending on the depth of in situ surveys, the percent of reef area covered with sUAS surveys and patchiness of the bleaching response. This study demonstrates the effective use of sUAS surveys for assessing the spatial dynamics of coral bleaching at colony-scale resolutions across entire patch reefs and evaluates the complementarity of data from both sUAS and in situ diver surveys to more accurately characterize the spatial ecology of coral communities on reef flats and slopes.

Topic Editor Dr. Line K. Bay

Electronic supplementary material The online version of this article (<https://doi.org/10.1007/s00338-018-1662-5>) contains supplementary material, which is available to authorized users.

✉ Joshua Levy
levyjosh@hawaii.edu

¹ Applied Research Laboratory, University of Hawaiʻi Mānoa, Honolulu, HI 96822, USA

² Department of Biology, University of Hawaiʻi Mānoa, Honolulu, HI 96822, USA

³ Porto University, Praça de Gomes Teixeira, 4099-002 Porto, Portugal

⁴ FlightWave (USA), Santa Monica, CA 90401, USA

⁵ Hawaiʻi Institute of Marine Biology, School of Ocean and Earth Science and Technology, University of Hawaiʻi Mānoa, Kaneohe, HI 96744, USA

Keywords sUAS · Mapping · Remote sensing · Coral reefs · Bleaching

Introduction

Coral reefs, which provide a variety of vital ecological and economical functions throughout tropical coastal communities, are in global decline due to a combination of coastal and global stressors (Bozec and Mumby 2015). Coral bleaching, usually caused by thermal stress, is widely known as one of the largest contributors to the global loss of coral reefs (Cesar et al. 2003; Baker et al. 2008; Normile 2016). In order to help understand the ecological impacts of the declining trend in global coral reef condition, it is essential to collect information at biologically relevant spatial scales to understand the spatial dynamics of coral bleaching.

Three major bleaching events have been documented in Kāneʻohe Bay, which occurred in 1996, 2014 and 2015 (Jokiel and Brown 2004; Bahr et al. 2015b). The September 2014 event was the most severe bleaching event documented in the Hawaiian Archipelago to date. Coral recovery was high within Kāneʻohe Bay, with the exception of reefs affected by a concurrent freshwater kill in July 2014 where recovery has been slow (Bahr et al. 2015a). Widespread coral bleaching was recorded again throughout Kāneʻohe Bay between the months of August and October 2015, again with high recovery throughout the bay (R Ritson-Williams, K Bahr pers. comm.).

Generally, coral bleaching surveys are conducted via in situ diver surveys or remote sensing techniques (Hedley et al. 2016). In situ diver surveys are necessary to obtain colony-level bleaching information. However, reef community structure and bleaching patterns can be heterogeneous over scales of centimeters to hundreds of meters, which make the small cumulative area of in situ diver assessments possibly unrepresentative of reef condition as a whole. Additionally, some reefs are situated where remoteness, weather conditions or reef topography prohibit the safe, routine collection of in situ reef information (Buddemeier and Smith 1999). Remote sensing surveys collect coral information over vast areas, but have temporal, spatial and monetary limitations that are particularly problematic when trying to answer coral bleaching questions at the colony level (Green et al. 1996; Hofmann and Gaines 2008). Unmanned aerial systems (UAS) or drones offer a viable alternative to traditional platforms for acquiring high-resolution remote sensing data at lower cost, increased operational flexibility and greater versatility (Watts et al. 2012; Udin and Ahmad 2014; Colefax et al. 2017). Small UAS (sUAS) are defined as fixed wing or multi-rotor aircraft that weigh less than 25 kg and are flown without a pilot in the cockpit (Hardin and Jensen 2011; Klemas 2015). sUAS have been used in several fields of coastal marine ecology including wildlife surveys, wetland assessments, coastal erosion assessments and coral reef surveys (Pierce et al. 2006; Martin et al. 2012; Hodgson et al. 2013, 2016; Casella et al. 2014, 2016; Flynn and Chapra 2014; Klemas 2015; Chirayath and Earle 2016). In this study, we utilized sUAS and photogrammetry techniques to create high-resolution maps (~ 1 cm ground sample distance from the waters surface) of four patch reefs in Kāneʻohe Bay, Hawaii, that were impacted by the 2014/2015 global coral bleaching event to determine the spatial dynamics of coral bleaching between and within patch reefs (PR). We also compared coral cover and coral bleaching metrics between aerial and in situ survey methodologies in efforts to validate aerial data accuracy and initiate the concept of integrating sUAS-derived and

in situ coral reef data, and bring attention to the benefits and limitations of both survey methodologies.

Methods

Study site

Kāneʻohe Bay, located on the northeastern side of Oʻahu, Hawaii, is the largest sheltered body of water in the main Hawaiian Islands and is characterized as a shallow, near-shore marine environment with well-developed fringing reefs and 57 distinct patch reefs, physically separated by sand/silt channels 10–12 m deep (Roy 1970; Bahr et al. 2015b). Patch reefs in Kāneʻohe Bay range from 1000 to 55,000 m², have reef flats less than 2 m below sea level and are located between 300 and 3000 m from the nearest shore (Roy 1970). These level, very shallow reef flats are ideal locations for sUAS surveys. During low-wind periods, Kāneʻohe Bay can experience very calm sea states and good visibility that are optimal for the successful use of sUAS surveys (Casella et al. 2016). During the Summer/Fall months of 2015, high atmospheric and ocean temperatures coincided with low winds to push nearshore temperatures above 30 °C, leading to extensive coral bleaching throughout Kāneʻohe Bay (R Ritson-Williams, K Bahr pers. comm.). We targeted four patch reefs (PR 20, PR 25, PR 42 and PR 44) for this study due to varied bleaching responses, positions in the Bay and size ranges of these reefs (2000–45,000 m²), which allowed us to optimize our survey techniques and compare results obtained with in situ methods (Fig. 1). This variation allowed us to optimize our survey techniques for different reef sizes and coral condition in efforts to develop a reef agnostic UAS survey protocol that can be easily adapted to reef sites beyond Kāneʻohe Bay.

The DJI Phantom 2, a low-cost, commercially available quad-rotor sUAS, was chosen for this study because of its relatively long flight time (~ 15 min), capacity to hold a 3-axis gimbal and 12-megapixel (MP) red–green–blue (RGB) sensor and compatibility with a flight planner. The 3-axis gimbal allowed for smooth, stable, imagery collection regardless of the pitch and yaw of the moving platform. A GoPro Hero 3 was a suitable RGB sensor due to its small size, lightweight and sufficient image resolution (12 MP). The GoPro was fitted with a circular polarizer to reduce glare artifacts as much as possible and programmed to collect a single 12 MP image two times per second during the flights. The DJI Ground Station (GS) was a free flight planner for iOS tablets that enabled the pilot to create up to 16 waypoints per flight on a satellite map-layer interface. Waypoints could be manually adjusted for location, height, time spent at waypoint, platform

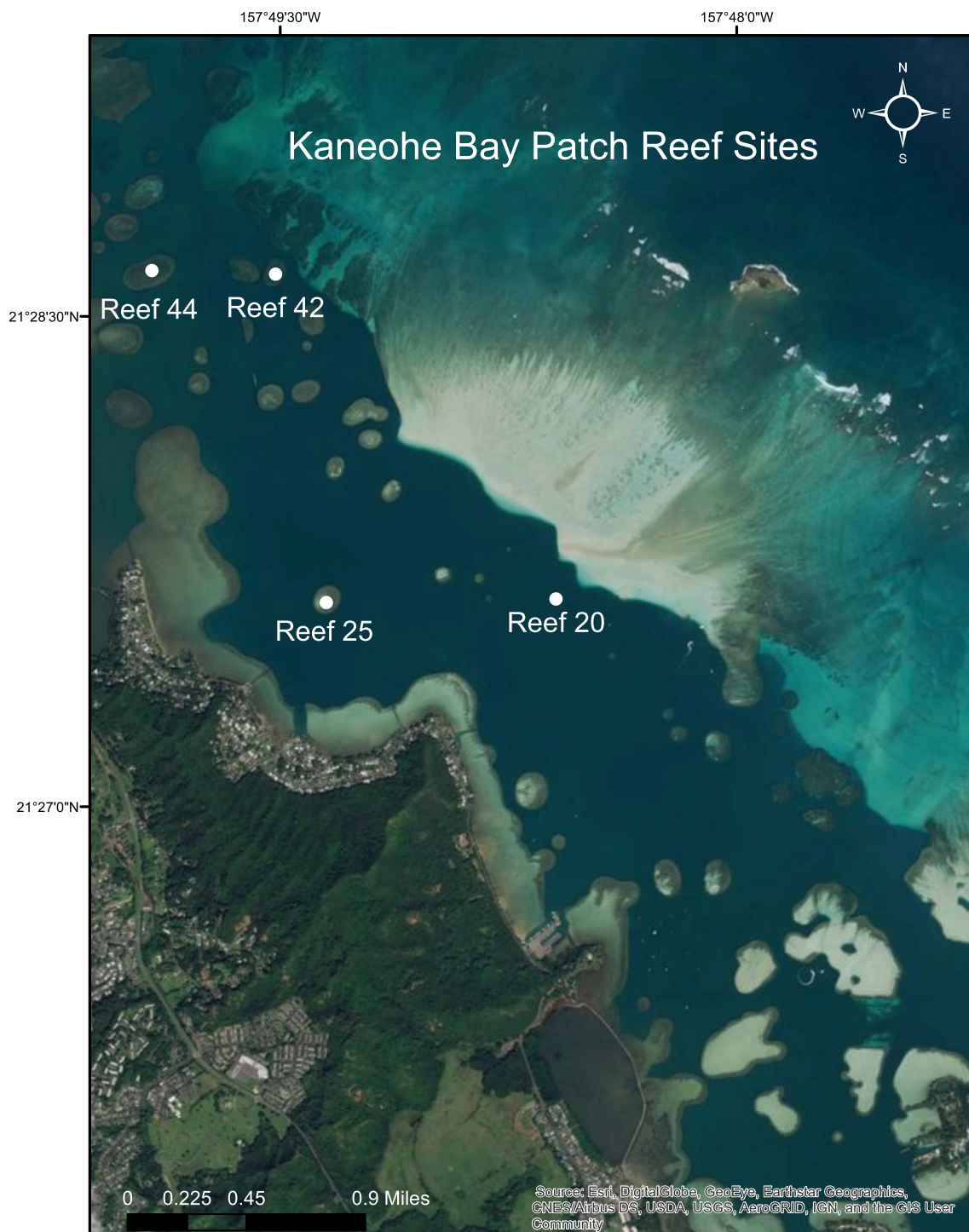
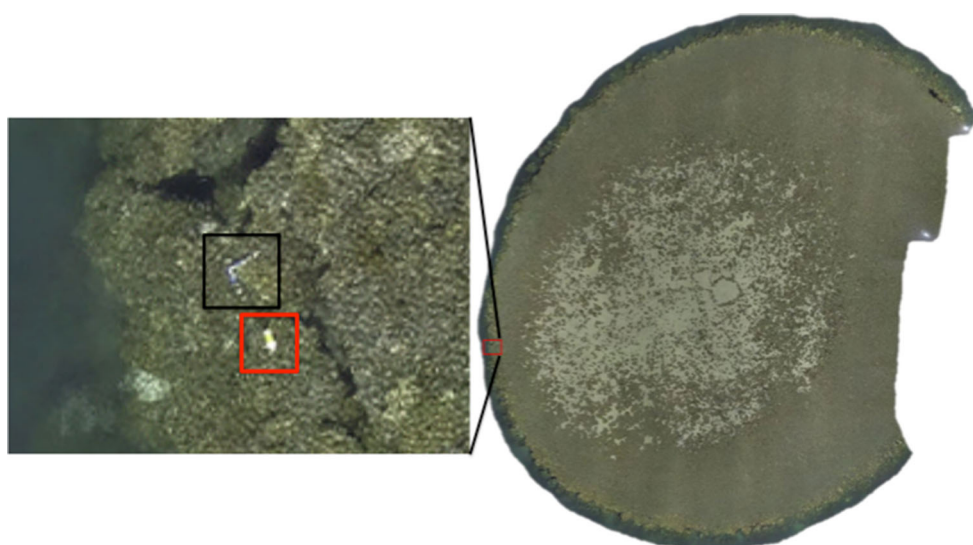


Fig. 1 Kāneʻohe Bay with the four targeted patch reefs indicated

orientation and speed between waypoints. The flight path was designed in a lawn mower pattern, allowing the sensor to travel over the reef, collecting still imagery at $\sim 70\%$ overlap in the x and y direction. The GoPro Hero 3 sensor has a field of view of 94° and 120° in the X and Y directions, respectively, in the “wide” setting. This meant that at

20 m altitude, the flight paths needed to be 15–20 m apart, and the camera must be traveling at a maximum ground speed of 5 m s^{-1} in order to collect sufficient overlap in the X and Y directions with a 2 FPS frame rate. Although the targeted image overlap was 70%, due to the rudimentary flight planner and UAS available at the time, flight path

Fig. 2 PR 25 with subset showing location of GCP and float. Cropped image showing GCP float (red box) and PVC marker (black box)



drift due to wind and GPS inaccuracies resulted in lower overlap in some areas.

Flights were flown at 15–20 m altitude to optimize image resolution. At lower altitudes (~ 10 –12 m), propeller-generated wind turbulence can impact the water state and produce distortion artifacts. Therefore, we found that for low-end multi-rotor sUAS such as the DJI Phantom series and a 12 MP sensor, a “happy medium” altitude of 15–20 m provided 0.8–1.0 cm ground sample distances (GSD) at the water surface, with no disturbance to the waters surface. Maximum flight time for the DJI Phantom 2 was ~ 15 min per battery and full reef coverage required between 0.5 and 5 batteries, depending on the reef size.

Preflight procedure

Prior to conducting sUAS assessments, we deployed ground control points (GCPs) in order to accurately georeference the reef imagery. Five floats and four L-shaped PVC pipes (0.34 m \times 0.34 m) distributed evenly along the reef perimeter were easily visible in the aerial imagery (Fig. 2). GPS coordinates of the GCPs were recorded for 1 min at each location with a Garmin GPSMap 76cx, which has a GPS Positional accuracy of < 10 m (Garmin 2009). The aircraft was launched in autopilot mode using the ground station.

All four sUAS reef assessments were conducted from the bow of a 17-ft Boston Whaler between 0830 and 1000 hrs. (HST). Early morning flights were necessary to reduce glare hotspots produced by high sun angle. The boat was anchored on the southeast side of each reef during sUAS operations, which prevented the pilot and spotter looking into the sun while monitoring the aircraft during flight. The spotter released the aircraft and monitored aircraft progress on the flight planner, while the pilot

maintained a visual on the aircraft during the entirety of the flight while holding the remote control. When the survey was completed, the pilot regained manual control and positioned the aircraft above the bow of the boat, to be retrieved by the spotter. Before each flight, the proper authorities at Marine Corps Base Hawaii (MCBH) and Honolulu International Airport were notified of flight locations, platform and time of flights in accordance with current FAA rulings at the time.

Partial to complete areas of each targeted patch reef were collected during the bleaching event, but, due to weather conditions, the collection of imagery of all reefs within a single morning was not possible. Imagery for Reef 44 was collected on August 23, 2015, while imagery for Reefs 42, 25 and 20 was collected between October 27, 2015, and October 29, 2015. Imagery was incomplete for three of the four reefs due to the combined effects of an inefficient flight planner and short UAS flight time, which limited the amount of area covered per flight. Although multiple batteries were used for each reef, we did not have enough batteries on hand to completely cover the entire area for the larger reefs. It is important to note that if conducting UAS surveys on fringing or barrier reefs, boat orientation may be less flexible and could require longer distances between the boat and UAS while conducting surveys. In addition to inconvenient orientation to the sun, wind and current directions that may make takeoff, maintaining visual contact with, and landing the UAS difficult. Prior to conducting UAS surveys, it is important to understand such environmental factors that may not be as important for in situ surveys.

Postprocessing

Aerial images for each reef were batch-edited in Adobe Lightroom to standardize color and increase shading contrast to improve the ability of the photogrammetry software to detect the necessary image features to successfully create an orthomosaic product. Agisoft Photoscan photogrammetry software was used to create orthomosaic models of partial to complete areas of each reef. This software uses structure from motion SfM techniques to identify points of interest between adjacent images to estimate the camera location at the collection point of each image, and then combines adjacent images to create dense point clouds and orthomosaic models of a complete scene (Stal et al. 2012). SfM techniques require at least 60% overlap between images in both the *X*- and *Y*-axes in order to decrease orthomosaic distortions (Stal et al. 2012). Prior to importing the images, the GoPro 3 was calibrated using Agisoft Lens, which characterizes the lens and creates a file that is used in Agisoft Photoscan to improve the estimated camera position accuracy. After uploading, the folder of single images is then “Aligned” at “High” accuracy using the “Generic” preselection. After alignment, camera positions were optimized using the “Optimize” tool and the orthomosaic was built using the “Mesh” as the surface and “Mosaic (default)” blending mode. RMS reprojection error was calculated as 4.05, 2.31, 3.08 and 2.44 pixels for PRs 20, 25, 42 and 44, respectively. This and other supplementary information in reference to orthomosaic model production can be found in supplementary material. Pixel size was calculated as $0.0110 \text{ m} \pm 0.005$ for all four orthomosaics. Models were then exported as TIFF files. It should be noted that Agisoft Photoscan has undergone several software updates since conducting this work, and therefore, some workflow procedures have changed, although the final products for each step remain the same. The orthomosaics were then georeferenced in ArcGIS using a combination of the GPS data from the GCP’s and visual references from base layer satellite imagery, which yielded a root mean square error (RMSE) of 0.5–0.8 pixels or 0.55–0.88 cm. A combination of both georeference aids was used because of the inaccuracy of the GCP GPS locations due to the relatively high error of the GPS (< 10 m) and the dynamic location of the CGP marker. The physical drift of the GCPs, yellow floats tied to anchors with ~ 1 m of rope, did not hold exact locations for the duration of deployment and therefore produced location errors that are a function of rope length, water depth and water/wind dynamics.

In situ ground-truthing was performed to evaluate the quality of the airborne imagery, utilizing $1 \text{ m} \times 1 \text{ m}$ photo-quadrats. The in situ photographs were not used for assessment of statistical accuracy, but rather for qualitative

comparisons that highlighted the airborne imagery’s ability to resolve different benthic types (Fig. 3a–c).

Image classification and spatial analysis

Image annotations were conducted manually in GIS software. The outline of each coral colony was digitized by hand to create individual polygons for each coral portion. Each polygon was assigned one of the three health states: pale, bleached and fully pigmented (healthy). Colonies that experienced partial bleaching or paling were divided into separate polygons. Non-coral cover such as sand, rubble and algae was not specifically cataloged, as these metrics were not relevant to the study, and as such were assigned to an “unclassified” category.

To assess the distribution of bleaching responses, all polygons for each health state were combined into a single polygon, producing three polygons (one of each health type) per reef. The area of each polygon was divided by total reef area to determine proportional cover for each coral health state, as well as total coral cover per reef. Each polygon was converted to point data, which was used to determine the distribution of each health type per reef. We examined the spatial autocorrelation of bleached, paled and healthy corals with Moran’s *I*, which uses feature locations to measure spatial autocorrelation, determining whether patterns are clustered, dispersed or randomly distributed, to determine the spatial distribution of each health state on each reef (Fischer 2010). We then conducted an optimized hot spot analysis to determine the location of high and low clumped areas of each health state on each reef (Fischer 2010). All spatial analyses were performed in ESRI ArcGIS version 10.3.1.

Coral cover comparison

The State of Hawai‘i Division of Aquatic Resources (DAR) conducted an assessment of Kaneohe Bay patch reefs in 2014 including PRs 20, 25, 42, 44 using an in situ “snap assessment” technique (Neilson et al. 2014). Surveyors, spaced approximately 5–10 m apart, swam transects across the reef and randomly placed a 0.5 m measuring stick every 5–10 m. At the location of the stick, GPS waypoints were collected, and percent live coral cover was estimated based on the benthic composition below the measuring stick (Neilson et al. 2014). Percent cover was categorized into 0, 1–10, 11–50 and 51–100% bins (Neilson et al. 2014). Surveys covered the entirety of each reef to depths of ≤ 3 m (Neilson et al. 2014). This method records point coral cover observations across a large portion of reef area and provided reef-wide coral cover values, which were used to compare against sUAS reef-wide coral cover survey results (Neilson et al. 2014).

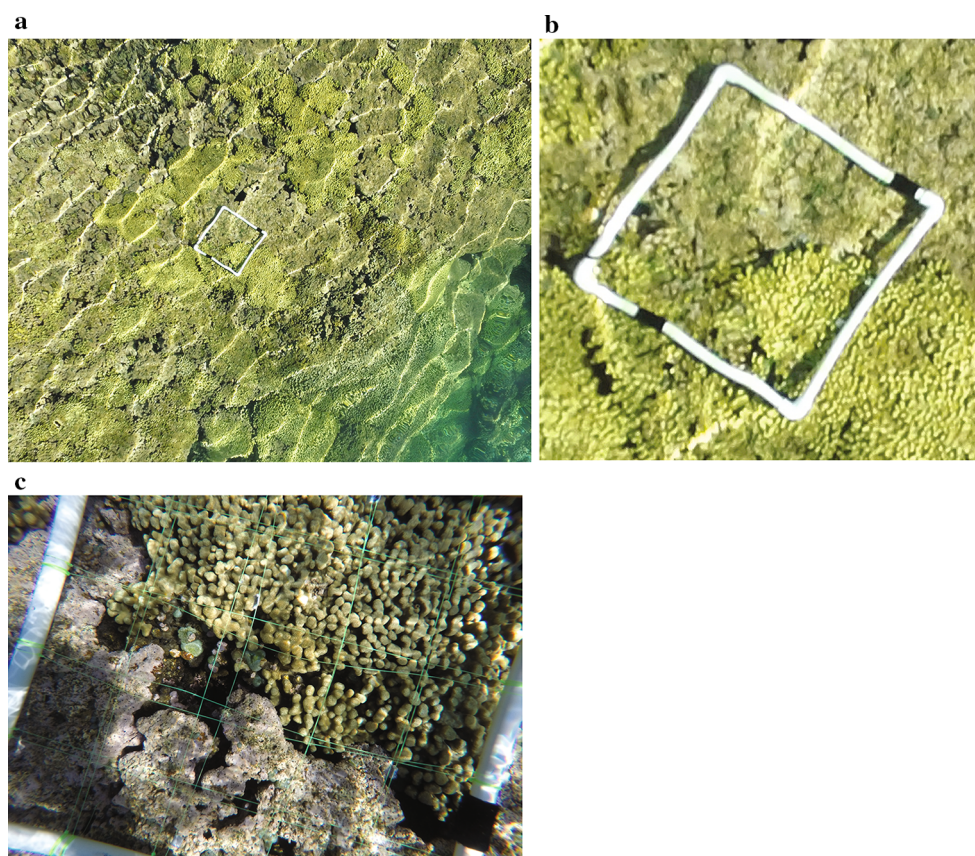


Fig. 3 Ground-truth verification of aerial imagery. **a** Aerial Image taken of healthy coral and non-coral substrate inside the 1 m² quadrat at 20 m altitude. **b** Cropped aerial image to isolate the quadrat. **c** In situ imagery of the quadrat. Note the insufficient image coverage of the in situ quadrat due to shallow reef depth

Coral bleaching comparison

In situ bleaching data were collected using underwater video of five, 10 m transects at 2 and 0.5 m depths on PRs 25, 42 and 44 on October 30, 2015 (Ritson-Williams unpublished). Transects were conducted on the west side of PR 25 and on the southwest corners of PRs 42 and 44 (Ritson-Williams unpublished) (Figs. 4a, 5a, 6a). Five still frames were randomly selected from each replicate transect per reef per depth and analyzed using Coral Point Count for Excel (Kohler and Gill 2006). Coral health values derived from transects were used to estimate percent coral bleaching on a reef-wide basis for each reef surveyed (Ritson-Williams unpublished). Percent bleaching values for each replicate transect per depth were averaged for each reef and compared to percent bleaching values calculated from the sUAS surveys.

All surveys were designed to estimate total coral cover/coral bleaching per patch reef. As such, precise horizontal accuracy for each data set is not required for a comparison between data sets as long as the compared surveys were conducted on the same patch reef.

Results

Spatial distribution of coral bleaching

Total coral cover varied significantly between the four patch reefs. The highest coral covers were on R20 and R42 with 56 and 55% cover, respectively (Table 1), while PR 25 had the lowest coral cover with 9.6% coral cover and PR 44 had 32.0% cover (Table 1). We pooled bleached and paled coral cover per reef into an “unhealthy” class to standardize coral cover by health for all four reefs. PR 44 had the largest percent of unhealthy coral cover with 45.4%, and PRs 20, 42 and 25 had relatively low percent unhealthy coral cover at 3.7, 6.9 and 2.2%, respectively (Table 1).

Bleached and paled corals on all reefs were classified as significantly clustered using Moran’s I spatial autocorrelation test with Z scores of 35.172, 31.506, 37.379 and 65.684 for PRs 20, 25, 42 and 44, respectively (Table 2). Unhealthy coral cover was clustered along the periphery of PR 25 in addition to an area in the center section of the reef flat (Fig. 5c). PRs 20 and 42 had the highest density of paled coral, clustered on the northeast (windward) and west

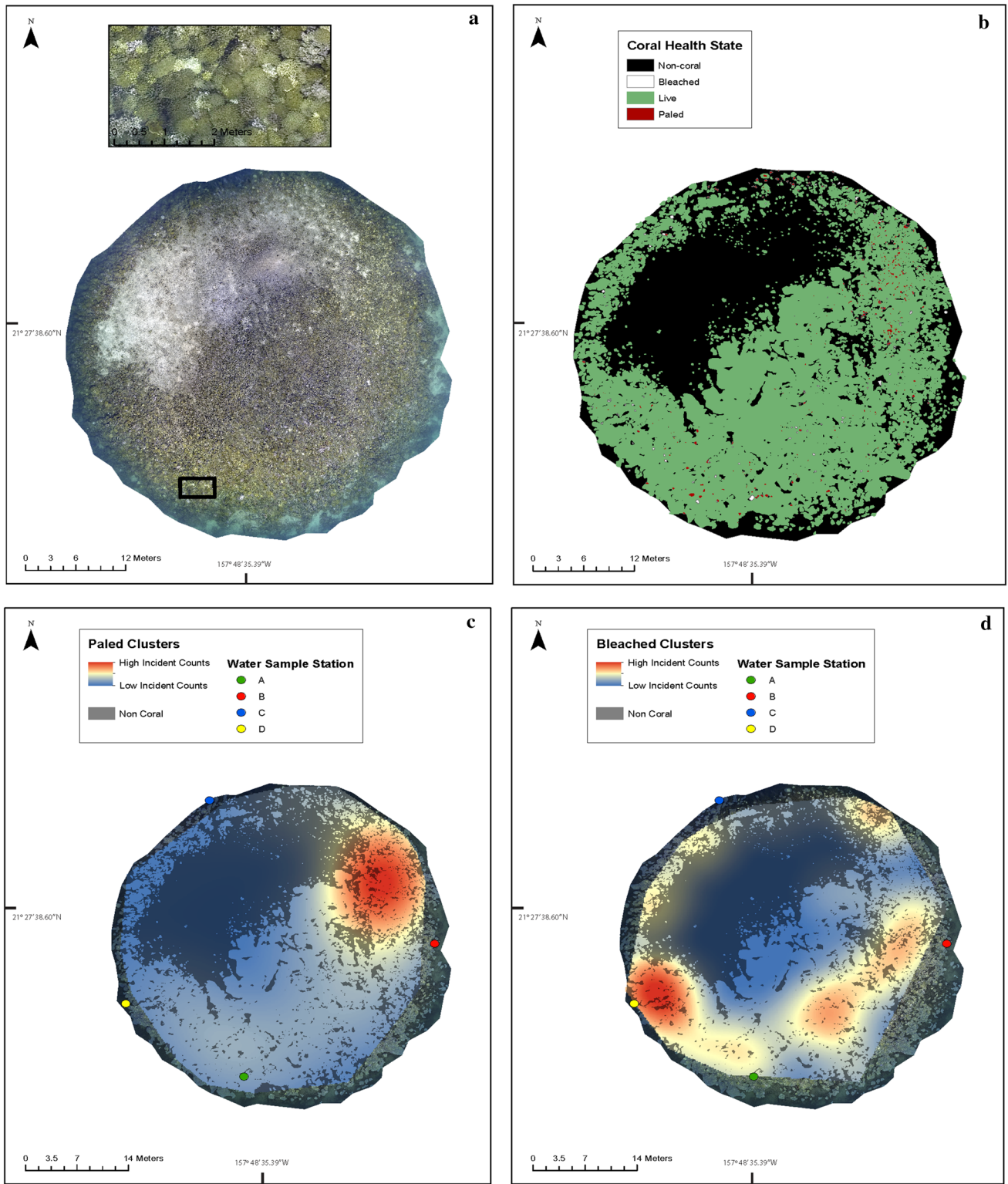


Fig. 4 Spatial analysis workflow for Reef 20. Pixel size: 0.009×0.009 m. **a** Reef mosaic with inset. **b** Orthomosaic classified into three coral health states and non-coral substrate. **c** Heat map of

paled colony clusters with environmental sample station locations. **d** Heat map of bleached colony clusters with water sample locations

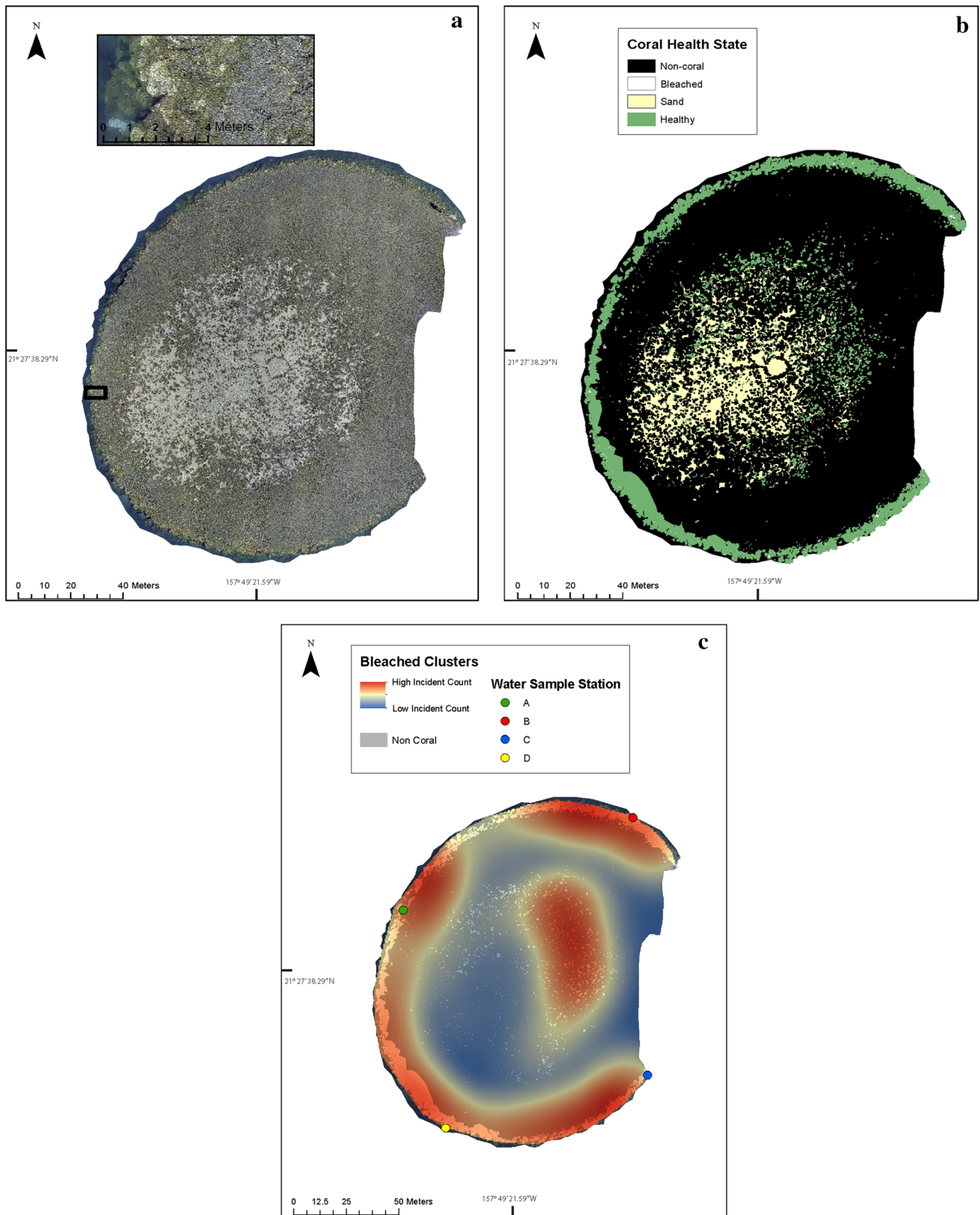


Fig. 5 Spatial analysis workflow for Reef 25. Pixel size: 0.033×0.033 m. **a** Reef mosaic with inset. Black oval represents general area where in situ coral bleaching surveys took place.

b Orthomosaic classified into two coral health states, sand and non-coral substrate. **c** Heat map of bleached colony clusters with environmental sample station locations

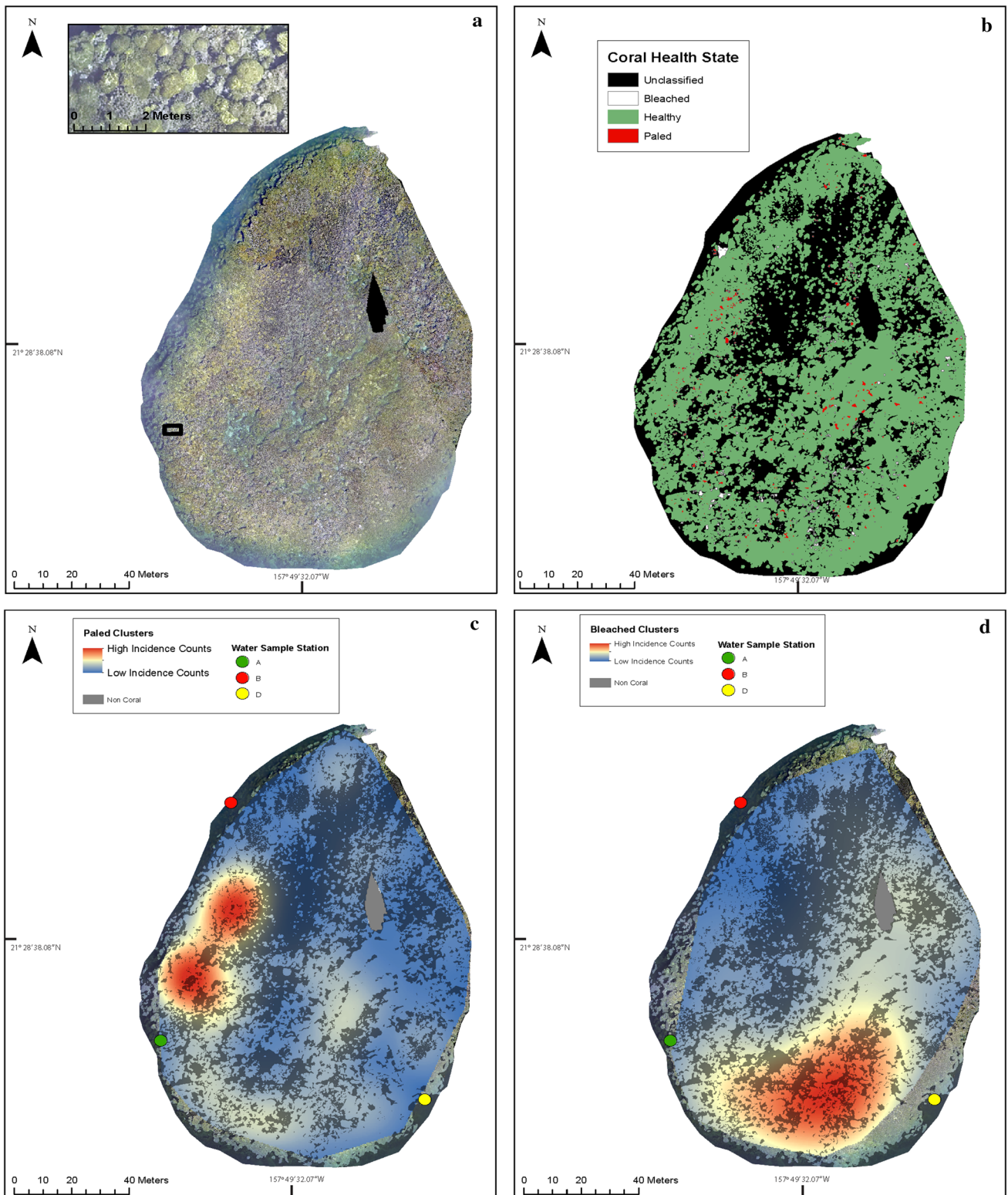


Fig. 6 Spatial analysis workflow for Reef 42. Pixel size: 0.021×0.021 m. **a** Reef mosaic with inset. Black oval represents general area where in situ coral bleaching surveys took place. **b** Orthomosaic classified into three coral health states and non-coral

substrate. **c** Heat map of paled colony clusters with environmental sample station locations. **d** Heat map of bleached colony clusters with water sample locations. Water sample station C was located beyond extent of reef imagery

Table 1 Coral cover categorized per reef by health type, total coral cover and total reef area covered by sUAS survey

Reef	Healthy (%)	Total coral cover (%)	Total reef cover (%)
20	97.77	54.97	100
25	93.09	9.61	78.5
42	96.29	56.03	94
44	54.57	32.03	52

“Unhealthy” and “healthy” cover percentages are calculated from total available coral cover for each reef

Table 2 Z scores and search thresholds for Moran’s I spatial autocorrelation test

Reef	Z score	Search threshold (m)
20	35.17	3.65
25	31.51	9.81
42	37.38	6.20
44	65.68	3.72

(leeward) side of each reef, respectively (Figs. 4c, 6c). Paled coral was more dispersed on Reef 44 although highest densities were located on the southern portion of the surveyed area (Fig. 7c). Bleached coral was dispersed throughout the periphery of PR 20, with higher-density clusters occurring on the southwest portion of the reef (Fig. 4d). There was a dense cluster of bleached coral on the southern portion of PR 42 (Fig. 6d) and on the southeast (windward) portion of PR 44 (Fig. 7d).

Coral cover comparison

When comparing the sUAS surveys to in situ diver surveys, coral cover differences ranged from 1 to 14% between the

two methods. The largest difference between coral cover occurred at PR 25, where sUAS surveys showed 14% lower coral cover than the in situ survey (Table 3). sUAS surveys overestimated coral cover on PRs 42 and 20 by 7 and 9%, respectively, while sUAS surveys underestimated coral cover on PR 44 by only 1% (Table 3).

Coral bleaching comparison

The largest difference in unhealthy coral cover between in situ and sUAS surveys occurred at PR 42, where sUAS surveys underestimated unhealthy coral cover by 45.4% compared to the average bleaching cover at both in situ survey depths (Table 4). At PR 44, differences between sUAS and in situ estimates of percent unhealthy coral cover were the lowest at 11.9% when averaging percent cover from the 0.5 and 2 m surveys (Table 4).

Discussion

Spatial analysis

Autocorrelation tests showed significantly clustered distributions for all reefs (Table 2) and clustering locations differed by reef and by health type (paled or bleached). For PRs 20, 42 and 44, heterogeneous distribution patterns of bleached and paled coral were between and within each reef (Figs. 4c, d, 6c, d, 7c, d). For Reefs 20 and 42, bleached and paled clusters did not overlap, and in the case of PR 20, high-density clusters of bleached and paled corals were located on opposite sides of the reef (Figs. 4c, d, 6c, d). Since PR 44 had a large percentage of unhealthy coral cover (Table 1), we expected to see a more uniform

Table 3 Patch reef coral cover comparing in situ and sUAS survey techniques

Reef	Total coral cover (%) (sUAS)	Estimated coral cover (%) (in situ)	Difference
44	32.03	33 (Range: 21.2–51.44)	0.97
42	56.03	49 (Range: 32.51–71.36)	7.03
25	9.61	24 (Range: 14.54–43.33)	14.39
20	54.97	46 (Range: 30.48–66.22)	8.97

In situ data were collected by DAR from February to April 2014²³. sUAS data were collected from August to October 2015

Table 4 Coral bleaching comparison between sUAS surveys and in situ surveys conducted at 0.5 and 2 m depth

Reef	Unhealthy (%) (sUAS)	Unhealthy (%) 2 m (in situ)	Difference (%) (sUAS vs. 2 m in situ)	Unhealthy (%) (0.5 m in situ)	Difference (%) (sUAS vs. 0.5 m in situ)	Difference (%) (sUAS vs. average of 0.5 and 2 m in situ)
44	45.43	44.38	1.05	68.22	22.79	11.92
42	3.71	45.37	41.67	52.79	49.08	45.39
25	6.91	42.55	35.65	54.92	48.02	41.84

In situ bleaching data were collected using video transects on October 30, 2015, as per Ritson-Williams unpublished

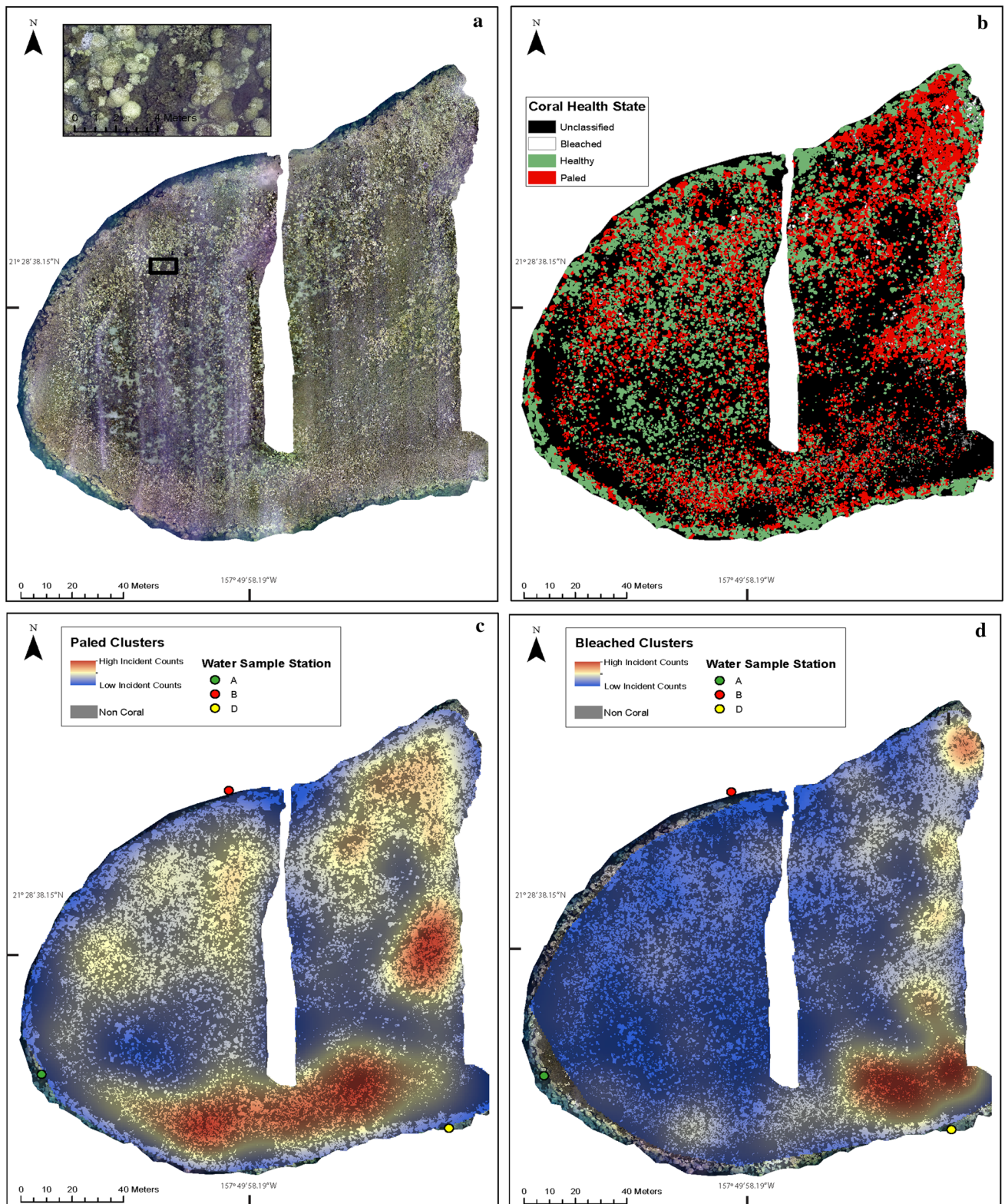


Fig. 7 Spatial analysis workflow for Reef 44. Pixel size: 0.007×0.007 m. **a** Reef mosaic with inset. Black oval represents general area where in situ bleaching surveys took place. **b** Orthomosaic classified into three coral health states and non-coral

substrate. **c** Heat map of paled colony clusters with environmental sample station locations. **d** Heat map of bleached colony clusters with water sample locations. Water sample station C was located beyond extent of reef imagery

distribution of unhealthy coral across this reef (Fig. 7c, d). However, the highest densities of both paled and bleached coral are located on the south/southeast portion of the surveyed area. The reasons for these heterogeneous, clumped distributions by reef and health type may stem from various environmental and physical variables that differed within and between patch reefs in Kāneʻohe Bay. PRs 20 and 42, which are located on the ocean side of the boat channel (Fig. 1), are more exposed to prevailing tidal and wind-driven currents that flush out nutrient and freshwater-rich coastal waters, which may exacerbate thermal stress, with low-nutrient oceanic water that protect corals from thermal stress (Hunter and Evans 1995; Baker et al. 2008; Lowe et al. 2009; Vega Thurber et al. 2014). The effects of these water masses may impact certain sides of the reefs more than others depending on the reef size and current direction, resulting in a clumped distribution of paled, bleached and fully pigmented corals. PR 44, which is located on the shore side of the bay, adjacent to a major stream output, may receive reduced oceanic flushing and experience more impacts from coastal stressors, resulting in higher overall paling and bleaching coral cover. A freshwater event in summer of 2014 caused significant mortality on the south, southwest portion of Reef 44 (Bahr et al. 2015a). The clustered bleaching and paling we saw in this location may be indicative of continued stress via coastal sources or perhaps residual effects of the freshwater event that indicates the system still has not completely recovered. Additionally, fine-scale changes in depth across each reef may introduce fine-scale refugia that are exposed to less irradiance stress, decreasing susceptibility of corals in those areas to bleaching (Brown 1997). Although temperature has been shown to vary within patch reefs, temperature data collected during the bleaching event did not vary significantly between reefs in Kāneʻohe Bay and was not shown to be a significant driver of coral bleaching (Gorospe and Karl 2011; Cunning et al. 2016). The spatial bleaching dynamics pose interesting questions in regard to the impacts of physical and environmental stressors on coral bleaching across various temporal and spatial scales.

Survey methodology comparison

Although the DAR data were collected ~ 1.5 yr prior to the sUAS surveys, these data sets still provide an interesting comparison between survey methods. The largest discrepancies in coral cover occurred between PRs 25 and 20, where we found coral cover on PR 25 was underrepresented by sUAS surveys, while coral cover on Reef 20 was overrepresented. The discrepancy in PR 25 coral cover values may be the result of high coral cover along the reef edge, which is difficult to capture via aerial imagery due to the inability to obtain oblique angles with UAS through the

water's surface, and large rubble and sand patches across the shallow reef flat, which is mostly inaccessible to snorkelers. PR 20 has a smaller sand patch on the reef flat and lower coral cover on the reef edge. It is also important to note that some of the sUAS surveys did not cover complete patch reefs due to insufficient image overlap and battery limitations. It is interesting that the most similar coral cover values between in situ and sUAS methodologies occurred on PR 44, which has the largest area and has the lowest percent reef area collected by sUAS surveys. The discrepancies in coral cover values between survey methods pose interesting results that support the need for both survey methods to accurately characterize patch reef flats and slopes. Further work could help determine the optimal reef survey area and survey method needed to efficiently and accurately characterize reef areas using in situ surveys when sUAS surveys are not feasible.

Coral bleaching comparison

The coral bleaching comparison illustrates how in situ survey accuracy can depend on the spatial distribution and heterogeneity of the bleaching event. The largest difference between coral cover values occurred at PR 42. The location of the in situ surveys conducted on Reef 42 appears to overlap with the area of highest density coral bleaching cover (Fig. 6a, d), which may have caused an overrepresentation of bleaching cover. Alternatively, Reef 44 has the smallest difference in percent unhealthy cover between sUAS and in situ surveys. The in situ surveys were located in a region of relatively low-density unhealthy coral cover (Fig. 7a, d), yielding a more accurate or possibly an underestimation of bleaching cover. Assessing the in situ surveys in relation to the locations of dense unhealthy coral cover visibly illustrates potential sampling limitations and biases that are inherent with small scale in situ surveys, which can be overcome with complimentary sUAS surveys. For this comparison study, we assumed the in situ values are more accurate than the sUAS values because in situ techniques are more established within the field of coral reef science. However, while we cannot confidently determine either survey method is more accurate than the other, this study highlights the need to further investigate utilizing both sUAS and in situ methods in efforts to improve the accuracy of coral reef assessments, and develop protocol for integrating various survey methods that increase the efficiency of collecting question-specific reef data.

Limitations

Although there are many benefits to incorporating sUAS surveys in coral reef science, there are still some

limitations that are inherent with remote sensing of benthic habitat through water. As the distance between the sensor and the substrate decreases, water artifacts such as distortions from waves become more pronounced. Wind-generated waves (0.1–2 s periods) are particularly disruptive, inhibiting the collection of accurate data at the colony level, and making benthic classifications challenging. In order to reduce the amount of wind-wave distortions, it is necessary to collect imagery on very low-wind days (1–7 KPH) or in protected bays where fetch is insufficient to produce substantial ripples. Additionally, imaging the benthos through a fluid lens produces inherent distortions, even in calm conditions, that impact fine-scale spatial details (Chirayath and Earle 2016).

Considering the use of sUAS in coral reef studies is still in its infancy, standardized protocols need to be developed and utilized in order to produce imagery that can be held to the same standard as traditional remote sensing data. Standards in sensor calibrations (although more important in projects working in the multi- and hyperspectral realm), lens calibrations and in situ validations are necessary in order to accurately and effectively compare results from UAS imagery over space and time.

The current lack of automated classification systems for high-resolution aerial RGB imagery is a serious bottleneck in data analysis efficiency. Due to the amount of area targeted with sUAS surveys, comprehensive manual benthic classifications are time-intensive. Although it is possible to distinguish between live coral and sand, the heterogeneity of both color and morphology within and between coral species makes classifications at the species level challenging when limited to RGB channels. Automated image processing and object identification can reduce data bottlenecks while maintaining accuracy requirements (Seymour et al. 2017). Such processes were attempted during this study, but inconsistencies in reflectance and texture values between inhibited accurate image classifications between reefs. As machine learning and neural networks become more robust, they will increase the efficiency of image processing, object detection and data management workflows that bottleneck of large data set projects. As with standard remote sensing techniques, the use of multi- and hyperspectral sensors on sUAS has the potential to vastly improve the efficiency and accuracy of benthic classifications (Hochberg and Atkinson 2003; Kutser et al. 2003).

Technology advancements

The development of technology within the UAS realm has and will continue to increase the efficiency of surveys and quality of data collected using sUAS. As reliability and efficiency of UAS platforms increase, we can conduct larger surveys in more remote locations. Advancements of

automation methods for image capture and processing will improve the accuracy and increase the range of conditions suitable for sUAS surveys. For example, Chirayath and Earle (2016) introduced a novel mathematical approach that utilizes the magnification distortion produced by wave peaks to magnify the target benthos while eliminating wind-wave distortions. This technique increases the number of possible flight days and locations beyond calm, protected environments, and increases the spatial resolution over uncorrected imagery 4–10 fold (Chirayath and Earle 2016).

Flight planners have advanced dramatically since 2015, where current systems such as eMotion, Mission Planner, DatuFly, Altizure and Drone Deploy allow the operator to easily create flight paths and monitor flights in real time. Sensors are getting smaller, cheaper and more powerful, allowing for the capture of higher-resolution imagery from smaller, lighter platforms that are fieldwork capable.

Future studies

Important next steps include correlating high spatial and temporal resolution sUAS-derived physical reef data with other data such as high spatial and temporal resolution environmental data to determine fine-scale patterns between coastal reef health and water quality. We also advocate for the development of protocol for integrating various survey methods that increase the efficiency of collecting question-specific reef data. As an intermediate spatial scale between in situ and satellite remote sensing data, UAS data can provide validation for traditional remote sensing at larger scales than previously capable with in situ methods and increase the efficiency of in situ work by providing unbiased colony resolution imagery over large areas.

Utility of high-resolution reef data from sUAS products can expand beyond coral bleaching applications in efforts to answer broader coral reef ecology questions. UAS-derived spatial data can be used in conjunction with traditional remote sensing techniques and in situ methods to understand coral species and morphology assemblages that may indicate cyclical stress events, identify suitable fish habitat and by association potential suitable sites for Marine Protected Areas (MPAs), quantify the spatial complexity of fine-scale shallow water depositional systems and map other indicators such as disease, physical impacts and macroalgae cover that increase our understanding of coral reef resilience (Purkis and Riegl 2005; Purkis et al. 2008, 2017; Rowlands et al. 2012; Knudby et al. 2013; Casella et al. 2016).

This study comprehensively documented spatial patterns of coral bleaching at centimeter-scale resolutions to examine colony-scale coral conditions across patch reefs and demonstrated the concept of using both sUAS and in situ survey as complementary methods to more

accurately characterize shallow reef flats and slopes. The high-resolution, reef-wide data set generated from the sUAS surveys allowed us to determine spatial characteristics of coral bleaching at a patch reef scale, which was previously unfeasible using current in situ surveys or traditional remote sensing techniques. This information can increase our understanding of coral bleaching events and illustrated the complexity of coral bleaching at these spatial scales. The high degree of versatility of sUAS makes them an ideal tool for reducing costs and increasing time efficiency of coral reef surveys while producing high-resolution data that have not been possible with previous remote sensing tools. The continued development of sUAS and autonomous software will continue to push the boundaries of the amount and type of coral reef information we can collect with these platforms in efforts to improve our understanding of coral reef dynamics at a range of spatial and temporal scales.

Acknowledgements Thanks to B. Neilson and the Division of Aquatic Resources team for giving us access to the in situ coral cover data. Thanks to R. Ritson-Williams for providing his in situ coral bleaching data. Thanks to T. Ralston for helping us navigate the FAA regulations. Funding was provided by NOAA award #NA10NMF4520163 (ECF). The University of Hawaii Graduate Student Organization provided funding to allow some of this work to be presented at the International Coral Reef Symposium. A special thanks to D. Kraft, B. Ellis, K. Bahr and M. Winston for their invaluable help in the field. This is SOEST contribution 10320 and HIMB contribution 1719.

Open Access This article is distributed under the terms of the Creative Commons Attribution 4.0 International License (<http://creativecommons.org/licenses/by/4.0/>), which permits unrestricted use, distribution, and reproduction in any medium, provided you give appropriate credit to the original author(s) and the source, provide a link to the Creative Commons license, and indicate if changes were made.

References

- Bahr KD, Jokiel PL, Rodgers KS (2015a) The 2014 coral bleaching and freshwater flood events in Kāneʻohe Bay, Hawaiʻi. *PeerJ* 3:e1136
- Bahr KD, Jokiel PL, Toonen RJ (2015b) The unnatural history of Kāneʻohe Bay: coral reef resilience in the face of centuries of anthropogenic impacts. *PeerJ* 3:e950
- Baker AC, Glynn PW, Riegl B (2008) Climate change and coral reef bleaching: An ecological assessment of long-term impacts, recovery trends and future outlook. *Estuar Coast Shelf Sci* 80:435–471
- Bozec YM, Mumby PJ (2015) Synergistic impacts of global warming on the resilience of coral reefs. *Proc R Soc B Biol Sci* 270. <https://doi.org/10.1098/rstb.2013.0267>
- Brown BE (1997) Coral bleaching: causes and consequences. *Coral Reefs* 16:129–138
- Buddemeier RW, Smith SV (1999) Coral adaptation and acclimatization: A most ingenious paradox. *Am Zool* 39:1–9
- Casella, E., A. Collin, D. Harris, S. Ferse, S. Bejarano, V. Parravicini, J. L. Hensch, and A. Rovere. 2016. Mapping coral reefs using consumer-grade drones and structure from motion photogrammetry techniques. *Coral Reefs* 1–7
- Casella E, Rovere A, Pedroncini A, Mucerino L, Casella M, Cusati LA, Vacchi M, Ferrari M, Firpo M (2014) Study of wave runup using numerical models and low-altitude aerial photogrammetry: A tool for coastal management. *Estuar Coast Shelf Sci* 149:160–167
- Cesar H, Burke L, Pet-soede L (2003) The economics of worldwide coral reef degradation. *Atlantic* 14:24
- Chirayath V, Earle S (2016) Drones that See Through Waves - Developing New Tools in Coastal Marine Conservation. *Aquat Conserv Mar Freshw Ecosyst Special Is.* <https://doi.org/10.1002/aqc.2654>
- Colefax AP, Butcher PA, Kelaher BP (2017) Review article The potential for unmanned aerial vehicles (UAVs) to conduct marine fauna surveys in place of manned aircraft. *ICES J Mar Sci.* <https://doi.org/10.1093/icesjms/fsx100>
- Cunning R, Ritson-Williams R, Gates R (2016) Patterns of bleaching and recovery of *Montipora capitata* in Kāneʻohe Bay, Hawaiʻi, USA. *Mar Ecol Prog Ser* 551:131–139
- Fischer, M. M. 2010. Handbook of Applied Spatial Analysis
- Flynn KF, Chapra SC (2014) Remote sensing of submerged aquatic vegetation in a shallow non-turbid river using an unmanned aerial vehicle. *Remote Sens* 6:12815–12836
- Garmin. 2009. GPSMAP 76Cx[®]
- Gorospe KD, Karl Sa (2011) Small-Scale Spatial Analysis of In Situ Sea Temperature throughout a Single Coral Patch Reef. *J Mar Biol* 2011:1–12
- Green EP, Mumby PJ, Edwards aJ, Clark CD (1996) A review of remote sensing for the assessment and management of tropical coastal resources. *Coast Manag* 24:1–40
- Hardin PJ, Jensen RR (2011) Small-Scale Unmanned Aerial Vehicles in Environmental Remote Sensing: Challenges and Opportunities. *GIScience Remote Sens* 48:99–111
- Hedley J, Roelfsema C, Chollett I, Harborne A, Heron S, Weeks S, Skirving W, Strong A, Eakin C, Christensen T, Ticzon V, Bejarano S, Mumby P (2016) Remote Sensing of Coral Reefs for Monitoring and Management: A Review. *Remote Sens* 8:118
- Hochberg EJ, Atkinson MJ (2003) Capabilities of remote sensors to classify coral, algae, and sand as pure and mixed spectra. *Remote Sens Environ* 85:174–189
- Hodgson A, Kelly N, Peel D (2013) Unmanned aerial vehicles (UAVs) for surveying Marine Fauna: A dugong case study. *PLoS One* 8:1–15
- Hodgson JC, Baylis SM, Mott R, Herrod A, Clarke RH (2016) Precision wildlife monitoring using unmanned aerial vehicles. *Sci Rep* 6:22574
- Hofmann GE, Gaines SD (2008) New Tools to Meet New Challenges: Emerging Technologies for Managing Marine Ecosystems for Resilience. *Bioscience* 58:43
- Hunter CL, Evans C (1995) Coral Reefs in Kaneohe Bay, Hawaii: Two centuries of western influence and two decades of data. *Bull Mar Sci* 57:501–515
- Jokiel PL, Brown EK (2004) Global warming, regional trends and inshore environmental conditions influence coral bleaching in Hawaii. *Glob Chang Biol* 10:1627–1641
- Klemas VV (2015) Coastal and Environmental Remote Sensing from Unmanned Aerial Vehicles: An Overview. *J Coast Res* 315:1260–1267
- Knudby A, Jupiter S, Roelfsema C, Lyons M, Phinn S (2013) Mapping coral reef resilience indicators using field and remotely sensed data. *Remote Sens* 5:1311–1334
- Kohler KE, Gill SM (2006) Coral Point Count with Excel extensions (CPCe): a visual basic program for the determination of coral

- and substrate coverage using random point count methodology. *Comput Geosci* 32:1259–1269
- Kutser T, Dekker AG, Skirving W (2003) Modeling spectral discrimination of Great Barrier Reef benthic communities by remote sensing instruments. *Limnol Oceanogr* 48:497–510
- Lowe RJ, Falter JL, Monismith SG, Atkinson MJ (2009) A numerical study of circulation in a coastal reef-lagoon system. *J Geophys Res Ocean* 114:1–18
- Martin J, Edwards HH, Burgess MA, Percival HF, Fagan DE, Gardner BE, Ortega-Ortiz JG, Ifju PG, Evers BS, Rambo TJ (2012) Estimating Distribution of Hidden Objects with Drones: From Tennis Balls to Manatees. *PLoS One* 7:e38882
- Neilson, B., J. Blodgett, C. Gewecke, B. Stubbs, and K. Tejchma. 2014. Kaneohe Bay, Oahu Snap-Assessment Report
- Normile, D. 2016. El Niño's warmth devastating reefs worldwide. *Science* (80-). **352**: 15 LP-16
- Pierce G, Iv J, Pearlstine LG, Percival HF (2006) An Assessment of Small Unmanned Aerial Vehicles for Wildlife Research. *BioOne* 34:750–758
- Purkis SJ, Graham N a J, Riegl BM (2008) Predictability of reef fish diversity and abundance using remote sensing data in Diego Garcia (Chagos Archipelago). *Coral Reefs* 27:167–178
- Purkis SJ, Kohler KE, Riegl BM, Rohmann SO (2017) The Statistics of Natural Shapes in Modern Coral Reef Landscapes. *J Geol* 115:493–508
- Purkis SJ, Riegl B (2005) Spatial and temporal dynamics of Arabian Gulf coral assemblages quantified from remote-sensing and in situ monitoring data. *Mar Ecol Prog Ser* 287:99–113
- Rowlands G, Purkis S, Riegl B, Metsamaa L, Bruckner A, Renaud P (2012) Satellite imaging coral reef resilience at regional scale. A case-study from Saudi Arabia. *Mar Pollut Bull* 64:1222–1237
- Roy, K. 1970. Change in Bathymetric Configuration, Kaneohe Bay, Oahu 1882–1969
- Seymour AC, Dale J, Hammill M, Halpin PN, Johnston DW (2017) Automated detection and enumeration of marine wildlife using unmanned aircraft systems (UAS) and thermal imagery. *Nat Publ Gr* 7:1–10
- Udin W, Ahmad A (2014) Assessment of Photogrammetric Mapping Accuracy Based on Variation Flying Altitude Using Unmanned Aerial Vehicle. *IOP Conf Ser Earth Environ Sci* 18:1–7
- Vega Thurber RL, Burkepile DE, Fuchs C, Shantz AA, McMinds R, Zaneveld JR (2014) Chronic nutrient enrichment increases prevalence and severity of coral disease and bleaching. *Glob Chang Biol* 20:544–554
- Watts AC, Ambrosia VG, Hinkley EA (2012) Unmanned aircraft systems in remote sensing and scientific research: Classification and considerations of use. *Remote Sens* 4:1671–1692